PROCEEDINGS of the
23rd International Congress on Acoustics

9 to 13 September 2019 in Aachen, Germany

Aeroacoustic and aerodynamic study of trailing-edge serrated airfoils in tandem configuration

Xiao Liu[1]; Syamir Alihan Showkat Ali[2]; Mahdi Azarpeyvand[3]; Yannick Mayer[4]

[1] Faculty of Engineering, University of Bristol, United Kingdom

[2] School of Manufacturing Engineering, University Malaysia Perlis, Malaysia

[3] Faculty of Engineering, Bristol University, United Kingdom

[4] Faculty of Engineering, Bristol University, United Kingdom

ABSTRACT

This paper presents a comprehensive experimental study on the application of trailing-edge serrations as a passive control method for reducing the unsteady aerodynamics loading and noise on airfoils in tandem configurations. The purpose of this study is to investigate the effectiveness of serrated trailing-edge on cambered NACA 65-710 airfoil to control and reduce the turbulent flow within the gap area between the two airfoils. The wake flow characteristics for an isolated cambered NACA 65-710 airfoil with and without the trailing-edge serration treatment have been carried out using two-dimensional Particle Image Velocimetry (PIV) method. The acoustic signature of the tandem airfoil is also presented for the near- and far-field noise measurements. Flow experiments were performed using sawtooth serration with different wavelength, for several tandem airfoil configurations (different airfoil gap distances). The results show that the use of serrations can generally lead to a significant reduction in the turbulent kinetic energy within the gap region, due to the interaction between the flows issued from the tip and root of the serration. The near- and far-field noise results have shown that a significant noise reduction can be achieved, especially with a sharp sawtooth serration.

Keywords: Passive Flow Control, Serration, Tandem Airfoil

1. INTRODUCTION

As the main component of turbines and compressors, the rotating blades are known to produce noise due to turbulent flow interactions of the rear-blade (i.e. stator) with the front-blade (i.e. rotor), which can be broadly categorized into trailing-edge, early separation and stall noise respectively [1]. However, studies of the aerodynamic noise produced by the rotating blades have prevailed as a challenging task over the past decades from both a theoretical perspective and a practical point of view. The principles of counter-rotating propeller noise were first investigated and analyzed in 1948 by Hubbard [2], which identified the dominant interference mechanisms and their associated noise production. Hanson [3] later reproduced and expanded some of Hubbard's findings. Using turbofan theory, he put forward that the interaction between the tip of the rear-blades and the wake flow resulted from the front propeller constitutes the major source of noise for the contra-rotating open rotor (CROR) propulsion systems. As such, it was inferred that minimizing wake turbulence intensity of the front blade could significantly reduce the overall noise signature of CROR systems. A computational study on the rudimentary effects of the unsteady interference between the airfoils in tandem configuration has been performed by Tuncer and Pletzer [4], and it was shown that the relative motion between the airfoils gave rise to the aerodynamic characteristics of the rear airfoil. In another

[1] xiao.liu@bristol.ac.uk
[2] syamir@unimap.edu.my
[3] m.azarpeyvand@bristol.ac.uk
[4] yannick.mayer@bristol.ac.uk

word, altering the relative position of the tandem airfoils changes the amount of wake turbulence (originating from the front blade) to which the rear airfoil interacts with and hence the aerodynamic noise generation.

In the past decade, reduction of trailing-edge noise through passive methods has been the focus of many studies, such as the use of serrated trailing-edge and surface treatment by porous materials and acoustic liners [5-20]. Serrated trailing-edges, in particular, have received significant interest due to its simple yet efficient noise reduction performance. The implementation of sawtooth and slotted-sawtooth serrated trailing-edge have shown to be effective in reducing the wake turbulence intensity and the corresponding noise generation, especially at high angles of attack where maximum aerodynamic performance is obtained [8, 13, 23]. The ability of serrated trailing-edge to reduce the turbulent energy content within the wake region can be associated with the highly three-dimensional flow originating from the tip- and root of the serration, making it an attractive solution to mitigate such wake-airfoil interaction noise for contra-rotating propellers and many other rotor-stator configurations

Compared to the aeroacoustic studies of a single airfoil, fewer measurements have been reported on two airfoils aligned in tandem configurations, not to mention airfoils with serrated trailing-edges. Hence, to better understand the effect of trailing-edge serration and the associated mechanisms of noise reduction, an extensive experimental study has been carried out on the aerodynamic and aeroacoustic performance of airfoils in tandem. In what follows, a detailed measurement on the wake development and near-/far-field noise generation have been undertaken and presented in this paper.

2. EXPERIMENTAL SETUP

2.1 Airfoil and Serration configurations

Figure 1 shows the schematic of the tandem airfoil configuration. The front and rear airfoils both had a chord length of $c = 150\,mm$ and a span of $l = 450\,mm$. While the front airfoil was manufactured from aluminum – 7075, the rear airfoil was made from RAKU-TOOL WB-1222 polyurethane board. To install the flat (baseline) and serration inserts at the trailing-edge , the front airfoil was designed with a $2.3\,mm$ blunt trailing-edge and a $15\,mm \times 0.8\,mm$ slot along the airfoil span, see Figure 1 (b). In order to have a comprehensive knowledge on the flow interactions, the rear airfoil was equipped with a total of 34 surface pressure taps on both the pressure and suction side of the airfoil, starting from the leading-edge (see Figure 1 (a)). The two airfoils were placed parallel to each other and rectangular endplates were used to maintain a nearly two-dimensional flow over the two airfoils. In the present work, two sawtooth serrations (Figure 2) were chosen based on its ability to reduce turbulent kinetic energy and noise as documented in [12, 14, 20]. The serration geometrical parameters are summarized in Table 1.

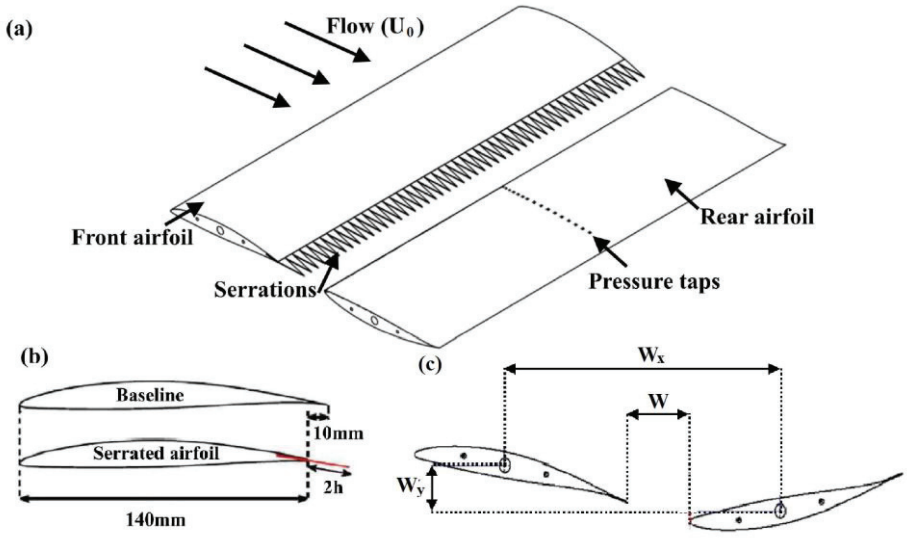

Figure 1 – The tandem airfoil configuration (a) Assembly view of front airfoil (NACA 65-710 with trailing-edge serration) and rear airfoil (NACA 65-710 with pressure taps distribution), (b) NACA 65-710 with and without trailing-edge serration, (c) Side view of the tandem airfoil arrangement

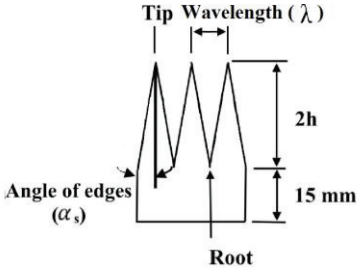

Figure 2 – Sawtooth serrations

Table 1 – Serration geometrical parameters

	2h (mm)	α_s (degree)	λ (mm)
Baseline	15	-	-
Wide sawtooth	30	22.5	24.8
Sharp sawtooth	30	8.53	9

The distance between the front and rear airfoil have been chosen as $W = 0.5c$ and $1.0c$ have been chosen for this study (see Figure 1(c)). The streamwise and vertical distance between the airfoil centre-points (W_x and W_y) were defined based on the locations where the maximum turbulent kinetic energy observed from the PIV results obtained for the baseline case of an isolated NACA 65-710 airfoil.

2.2 Experimental setup

In the present study, both the characterization of wake and near-field surface pressure measurements were carried out in the low turbulence tunnel at University of Bristol. Two-component Particle-Image Velocimetry was used to determine the wake development and energy contents of an isolated airfoil with and without the trailing-edge serration. A $1\,mm$-thick laser sheet was illuminated by Dantec DualPower $200\,mJ$ Nd:YAG laser with wavelength of $532\,nm$ and a repetition rate of $15\,Hz$. The time delay between the two consecutive laser pulses was set to $23\,\mu s$, to ensure adequate particle shifts within the final interrogation window. A mixture of Polyethylene glycol 80 was atomized to produce seeding with mean particle diameters of $1\,\mu m$. For each case, a total of 1600 images pairs, captured by a FlowSense EO 4M CCD camera ($2048 \times 2048\,pixels^2$), were analyzed using DynamicStudio, with a field of view of $148\,mm \times 148mm$. The iterative process yielded final correlation windows of $16\,pixels \times 16\,pixels$ ($\sim 1.1 \times 1.1\,mm^2$) with an overlap of 50% producing a vector spacing of approximately $0.6\,mm$.

Near-field surface pressure fluctuations were measured using 34 remote Panasonic WM-61A microphones connected to the brass tubes using plastic tubing with an inner and outer diameter of $0.8\,mm$ and $3.6\,mm$ respectively. The calibration of the remote sensing probe was based on the procedure described in Elsahhar *et al.* [21]. The unsteady pressure data were acquired by a National Instruments PX1e-4499 for a period of 16 seconds with a sampling rate of $2^{16}\,Hz$.

Far-field noise test was carried out in the University of Bristol's aeroacoustic facility, which is a closed-circuit, open-jet anechoic wind tunnel. The experiments in this study were performed at flow velocities $30\,m/s$ with turbulence intensity levels below 0.2% [22]. Signals from an array of 23 microphones mounted on an arc above the test rig were acquired by PXIe-4499 data acquisition card. The arc was designed to extend from angles 40° to 135° in steps of 5°, and similar to near-field measurement, the sampling frequency and duration remained as $2^{16}\,Hz$ and 16 seconds, to ensure data convergence. The power spectral density results for near- and far-field measurements were later calculated via Welch's method with a window size of 2^{14} samples, a Hamming window with 50% overlap and normalized with reference pressure of $p_0 = 20\,\mu Pa$.

3. RESULTS AND DISCUSSIONS

3.1 NACA 65-710 Airfoil Wake Measurements

To have a better understanding on the effects of the trailing-edge serrations on the wake development of the airfoil, PIV measurements of an isolated NACA 65-710 airfoil with the baseline and two sawtooth serrations ($\lambda = 9\,mm$ and $24.8\,mm$) have been carried out at angles of attack, $\alpha = 0^\circ, 5^\circ, 10^\circ$ and 15° for the flow velocity of $U_0 = 30\,m/s$. The fields of view used in our experiments covered the downstream locations $x/c = 0.2$ to 1, relative to the trailing-edge of the baseline case. It is crucial to highlight that the turbulence kinetic energy (TKE) maps of the isolated airfoil were then used to define the location of the rear airfoil (in red circle in Figure 3) for the noise generation studies.

Similar to the experiments reported by Xiao *et al.* [13], at $\alpha = 10^\circ$, implementation of trailing-edge

serration significantly modifies the turbulent kinetic energy (TKE) results, for both the wide sawtooth serration ($\lambda = 24.8\,mm$) in Figure 3(a) and sharp sawtooth serration ($\lambda = 9\,mm$) in Figure 3(b), under the present investigation. By applying a wide sawtooth serration, the wake TKE result for serration root shows a strong upward deflection and a thinner wake profile as compared with the baseline case. This is possibly due to the flow moving over the pressure side of the airfoil through the valley of the serration. Notably different from the root flow, the trend for tip flow is similar to that of the baseline case with small, and yet noticeable downward deflection. More importantly, when the sharp serration is applied, a significant TKE reduction (up to approximate 55%) can be observed in the wake TKE profile (see Figure 3(b)) with the profiles converge rapidly between the tip and the root after $x = 0.5c$.

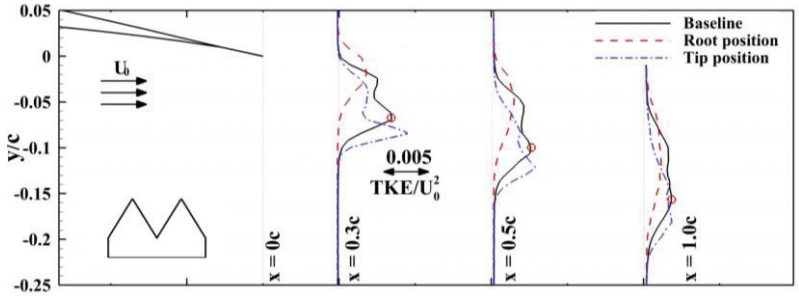

(a) wide sawtooth serration

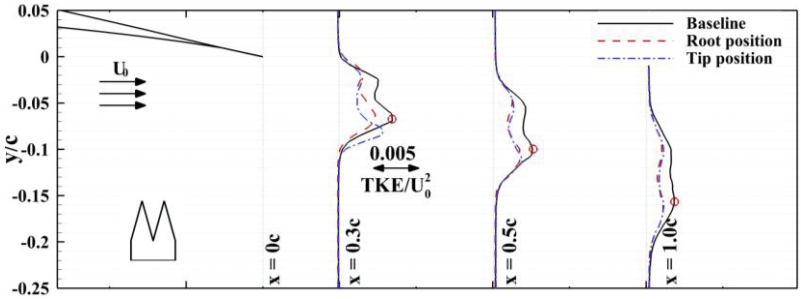

(b) sharp sawtooth serration

Figure 3 – Wake TKE profiles for isolated NACA65710 airfoil with different serrations at $\alpha = 10^{\circ}$ and $U_0 = 30\,m/s$. (a) wide sawtooth serration ($\lambda = 24.8\,mm$) (a) sharp sawtooth serration ($\lambda = 9\,mm$)

3.2 Near- and Far-field acoustic measurements

In order to further investigate the effectiveness of serration treatments for reducing the unsteady aerodynamic loading on the airfoil and radiated noise, surface pressure fluctuation measurements have been performed on the rear airfoil using the remote sensing method. In the tandem airfoil configurations, the front airfoil was fitted with baseline and different sawtooth serrations while the rear airfoils were placed at two different downstream locations, having gap distance of $W = 0.5c$ and $1c$, respectively.

The power spectral density (PSD) of the surface pressure fluctuations acting on the suction side of the airfoil is shown in Figure 4.With the gap distance of W=0.5c in Figure 4(a), wide sawtooth serration (top row) leads to a considerable increase of the pressure fluctuation energy over a wide range of frequency, within the leading-edge area of $x/c < 0.1$. It can also be observed that sharp sawtooth serration (bottom row) resulted in a slightly decreased surface pressure PSD at low frequencies ($fc/U_0 < 0.7$). Furthermore, the surface pressure PSD remains to be noticeably higher along the root position than those at tip position. Moving downstream to $x/c > 0.1$, the use of trailing-edge serrations resulted in a clear reduction (around $5\,dB$ at $x/c = 0.533$) of unsteady loading on the rear airfoil at frequency range $fc/U_0 < 0.7$. Unlike the wide sawtooth serration case, a small reduction of the surface pressure PSD can be observed, which begins immediately from the leading-edge and persists beyond $x/c = 0.233$. Interestingly, there is not much difference between the serration tip and root positions. Moreover, as observed from the results, trailing-edge serrations do not particularly benefit in the high frequency region of the pressure spectra. On contrary, an increase in the surface pressure PSD can be clearly seen at the leading-edge region for both serrated cases.

The surface pressure PSD results for the tandem airfoil configuration with the separation gap of $W = 1c$ are presented in Figure 4(b). The result of surface pressure PSD for wide sawtooth serration

shows similar trend to that of smaller separation gap distance, but larger surface pressure PSD reduction (up to $7\,dB$) at downstream chordwise locations. For sharp sawtooth serration, it can be observed that a reduction of the unsteady loading (up to $4\,dB$) on the rear airfoil over almost the whole suction side of the airfoil at frequency range of $fc/U_0 < 0.7$.

The results observed here is of great interest as the noise radiated from the rear airfoil is directly related to the unsteady pressure exerted on the airfoil and trailing-edge serrations on the front airfoil can modify significantly the overall unsteady pressure field experienced by the rear airfoil in the tandem configurations, and therefore the production of airfoil noise.

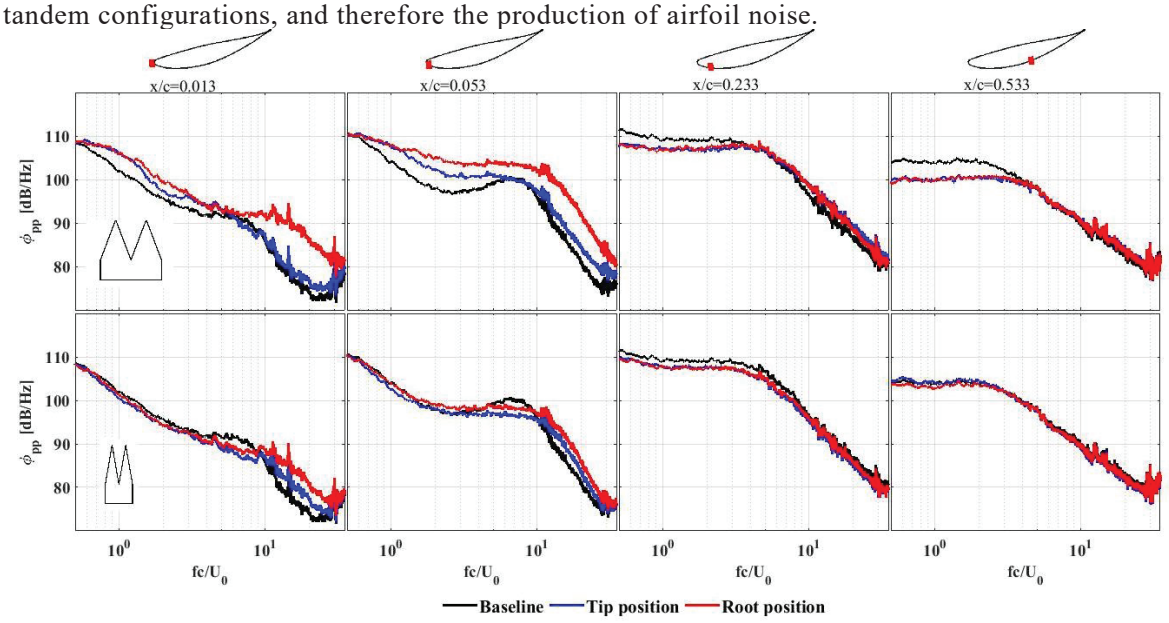

(a) W=0.5c

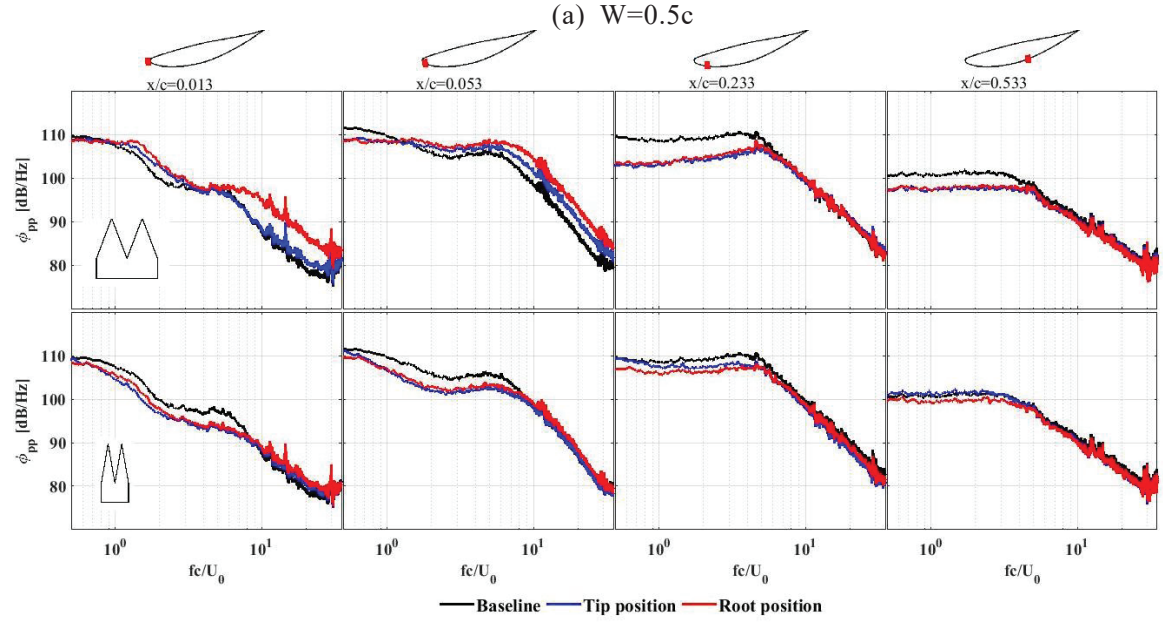

(b) W=1.0c

Figure 4 – Power spectral density of surface pressure fluctuation on the rear airfoil at $\alpha = 10^{\circ}$ and $U_0 = 30\,m/s$. (a) airfoil separation distance of W=0.5c (b) airfoil separation distance of W=1.0c

In order to better illustrate the effect of serrations, Figure 5 shows the contour map of the near-field coherence between the remote microphone 1 (first microphone on the suction side of the rear airfoil) and all other microphones at angle of attack $\alpha = 10^{\circ}$ and $U_0 = 30\,m/s$ with the gap distance between the front and rear airfoil of $W = 1c$. The positive x/c represents the coherence results along the suction side of the rear airfoil while negative x/c the pressure side of the rear airfoil.

The coherence map for the baseline case in Figure 5(a) shows a high coherence region in the whole

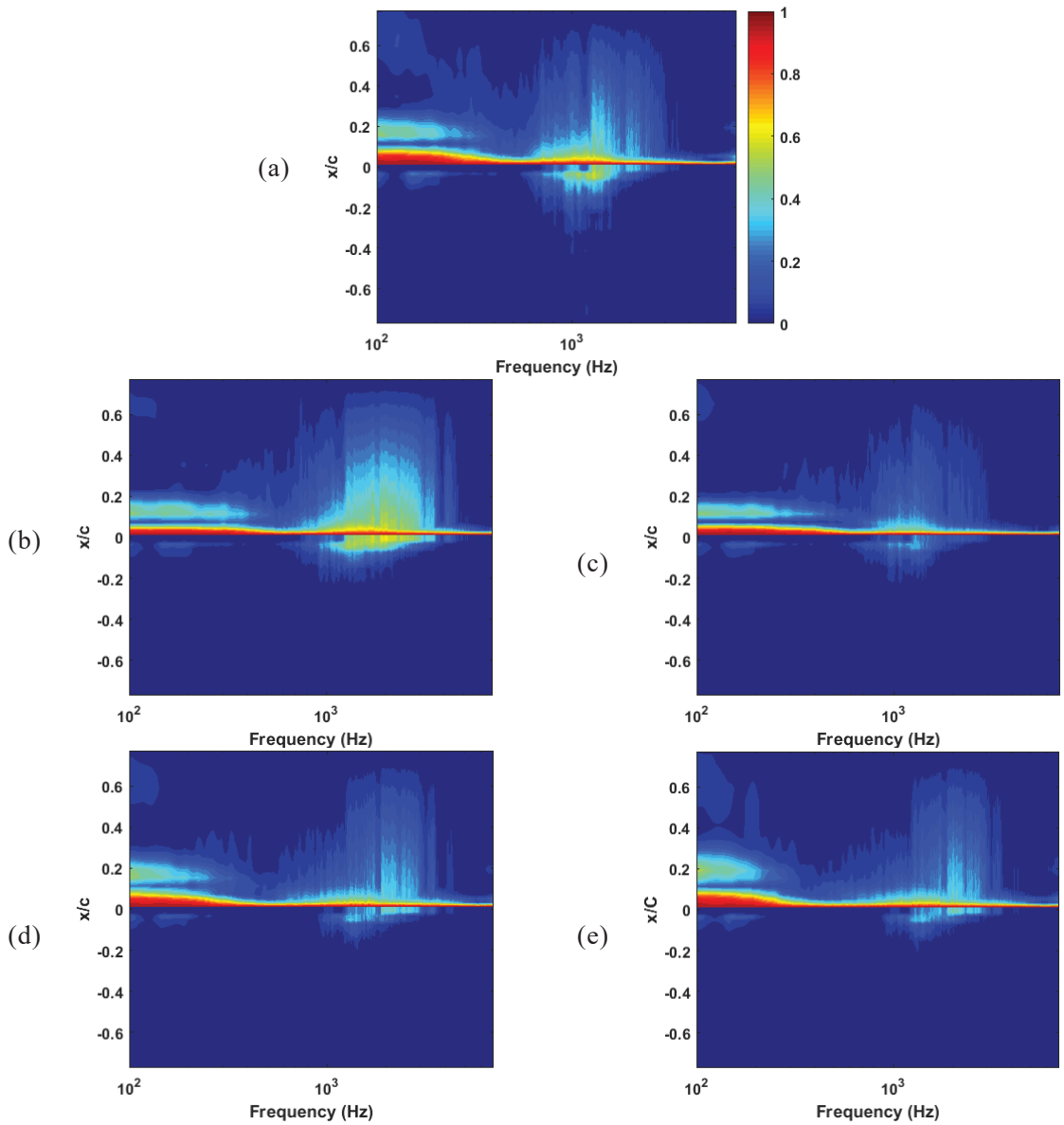

Figure 5 – Contour map of near-field coherence of first microphone on suction side with all other microphones ($W = 1c$):
(a) baseline (b) wide sawtooth – tip (c) wide sawtooth – root
(d) sharp sawtooth – tip (e) sharp sawtooth – root

frequency range near leading-edge area ($0 < x/c < 0.03$). At low frequency range ($f < 320\,Hz$), a high coherence area can also be found to exist between $0.1 < x/c < 0.25$. While at higher frequency range, $560\,Hz < f < 3.2\,kHz$, high coherence value between first and the rest of the remote sensors along the suction side of the airfoil can be observed to extend beyond half of the chord length ($x/c > 0.5$). At a similar frequency range, an elevated region of coherence can also be observed along the pressure side until approximately $x/c = 0.2$.

Figure 5(b) and 5(c) show the contour map of the near-field coherence for wide sawtooth serration case. At low frequency for both root (Figure 5(b)) and tip (Figure 5(c)) positions, high coherence value region can be found, similar to that of the baseline case. However, in the high frequency region, higher coherence, which is present along with the root position (and baseline), becomes noticeably attenuated. On the other hand, the results for the sharp sawtooth case, show no obvious difference between the root (Figure 5(d)) and tip position (5(e)) but clear reduction when compared with the baseline case at high frequency range ($560\,Hz < f < 3.2\,kHz$). Furthermore, it appears that the coherence spreads further downstream for the sharp sawtooth serration at low frequency range of $f < 320\,Hz$. Results from coherence clearly suggest that the reduction in the unsteady airfoil loading leads directly to a loss of coherence, and hence possibly better mixing for the near-field flow structures.

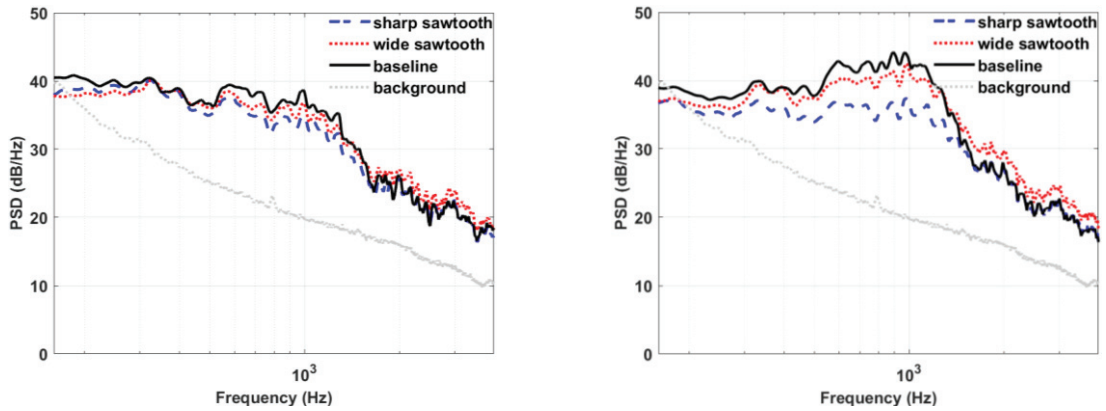

(a) W= 0.5c (b) W= 1.0c

Figure 6 – Power spectral density of the far-field noise measurements. (a) airfoil separation distance of W=0.5c (b) airfoil separation distance of W=1.0c

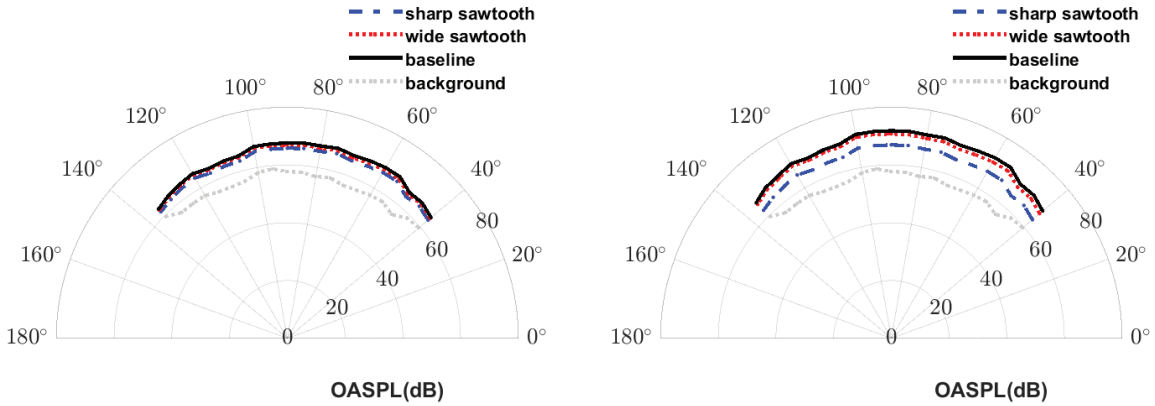

(a) W= 0.5c (b) W=1.0c

Figure 7 – Overall sound-pressure-level directivity patterns. (a) airfoil separation distance of W=0.5c (b) airfoil separation distance of W=1.0c

Figure 6 shows the far field noise measured at $30\,m/s$ over the tandem airfoil configuration with two gap distances of $W = 0.5c$ (in Figure 6(a)) and $W = 1c$ (in Figure 6(b)). For clarity and reference, the background noise is shown in grey in the figures. In Figure 6(a), when compared with the baseline case, the far-field PSD demonstrates that trailing-edge serration can lead to a small decrease in the airfoil noise with frequency lower than $1.5\,kHz$ for both serration cases, although the sharp sawtooth produces an additional $0.5 - 2\,dB$ reduction than the wide sawtooth. At a higher frequency range ($1.5\,kHz < f < 4\,kHz$) the far-field PSD for the serrated case resulted in a similar magnitude and trend, as the baseline case. When increase the distance between two airfoils to $W = 1c$ (see Figure 6(b)), the result for wide sawtooth serration exhibits a small noise reduction, similar to that observed at $W = 0.5c$ gap distance. However, for sharp sawtooth serration, a much more significant noise reduction (up to 11 dB) can be identified, which the broadband hump has been considerably reduced with a frequency range of $300\,Hz < f < 1.5\,kHz$.

Figure 7 presents the overall sound-pressure-level (OASPL) directivity pattern for the baseline case and trailing-edge serrated cases for two different gap distances ($W = 0.5c$ and $1c$) at $U_0 = 30\,m/s$. Figure 7(a) shows that both serration geometries slightly reduce the noise levels to that of the baseline case at all angular locations, with the sharp sawtooth serration outperforming the wide sawtooth. In Figure 7(b), as compared with the baseline case, the OASPL results for the wide sawtooth serrated cases remain similar in trend to that of the results in 7(a) across all angular directive range while the sharp sawtooth serrated case produces an approximately 5 dB reduction.

4. CONCLUSIONS

The present study demonstrates that the use of trailing-edge serration can significantly change the wake flow profiles through enhancing the flow mixing between the pressure and suction side of the airfoil, which leads to a faster TKE decay. Based on the TKE decay, applying a trailing-edge serration

on the front airfoil in tandem airfoil configurations will reduce the incoming TKE level for the leading-edge of the rear airfoil. This prone to produce a significant noise decrease (up to 9 dB) at the frequency lower than 1.5 kHz. The near-field surface pressure measurement and coherence map for serrated cases also show a clear reduction of unsteady aerodynamic loading, and hence airfoil noise, when compared with the unserrated baseline case. A comparison between two serrations shows that sharp sawtooth configuration produces a more desirable reduction in the near-field loads, which translates into a greater far-field noise reduction.

REFERENCES

1. T. Brooks, D. Pope, M. Marcolini, Airfoil self-noise and prediction, in: NASA-RP-1218, 1989.
2. H. H. Hubbard, Sound from dual-rotating and multiple single-rotating propellers, NACA TN 1654.
3. D. B. Hanson, Noise of counter-rotation propellers, Journal of Aircraft, 22 (7) (1985) 609–617.
4. I. Tuncer, M. Platzer, Analysis of unsteady airfoil interference effects using a zonal navier-stokes solver, in: 33rd Aerospace Sciences Meeting and Exhibit, 1995, p. 307.
5. R. Sandberg, L. Jones, Direct numerical simulations of low reynolds number flow over airfoils with trailing-edge serrations, Journal of Sound and Vibration 330 (16) (2011) 3818–3831.
6. T. P. Chong, P. F. Joseph, An experimental study of airfoil instability tonal noise with trailing edge serrations, Journal of Sound and Vibration 332 (24) (2013) 6335–6358.
7. M. Azarpeyvand, M. Gruber, P. Joseph, An analytical investigation of trailing edge noise reduction using novel serrations, in: 19th AIAA/CEAS Aeroacoustics Conference, AIAA 2013-2009.
8. M. Gruber, Aerofoil noise reduction by edge treatments, Doctoral thesis, University of Southampton (2012).
9. D. Moreau, L. Brooks, C. Doolan, On the noise reduction mechanism of a flat plate serrated trailing edge at low-to-moderate reynolds number, in: 18th AIAA/CEAS aeroacoustics conference, AIAA 2012-2186.
10. T. Chong, P. Joseph, M. Gruber, Airfoil self noise reduction by non-flat plate type trailing edge serrations, Applied Acoustics 74 (4) (2013) 607–613.
11. F. Avallone, C. Arce Leon, S. Pr¨obsting, K. P. Lynch, D. Ragni, Tomographic-PIV investigation of the flow over serrated trailing-edges, in: 54th AIAA Aerospace Sciences Meeting, AIAA 2016-1012.
12. L. Ji, W. Qiao, F. Tong, K. Xu, W. Chen, Experimental and numerical study on noise reduction mechanisms of the airfoil with serrated trailing edge, in: 20th AIAA/CEAS Aeroacoustics Conference, AIAA 2014-3297.
13. X. Liu, M. Azarpeyvand, R. Theunissen, Aerodynamic and aeroacoustic performance of serrated airfoils, in: 21st AIAA/CEAS Aeroacoustics Conference, AIAA 2015-2201.
14. S. A. Showkat Ali, X. Liu, M. Azarpeyvand, Bluff body flow and noise control using porous media, in: 22nd AIAA/CEAS Aeroacoustics Conference, AIAA 2016-2754.
15. S. A. Showkat Ali, M. Azarpeyvand, C. R. I. da Silva, Trailing-edge flow and noise control using porous treatments, Journal of Fluid Mechanics, 850 (2018) 83-119.
16. S. A. Showkat Ali, M. Azarpeyvand, M. Szoke, C. R. I. da Silva Boundary layer flow interaction with a permeable wall, Physics of Fluids, 30 (2018) 085-111.
17. S. A. Showkat Ali, M. Azarpeyvand, C. R. I. da Silva, Experimental Study of Porous Treatment for Aerodynamic and Aeroacoustic Purposes, in: 23rd AIAA/CEAS Aeroacoustics Conference, AIAA 2017-3358.
18. S. A. Showkat Ali, M. Azarpeyvand, M. Szoke, C. R. I. da Silva, Turbulent Flow Interaction with Porous Surfaces, in: 24th AIAA/CEAS Aeroacoustics Conference, AIAA 2018-2801.
19. A. Afshari, M. Azarpeyvand, A. A. Dehghan, M. Szoke, Trailing edge noise reduction using novel surface treatments, in: 22nd AIAA/CEAS Aeroacoustics Conference, AIAA 2016-2384.
20. Q. Ai, M. Azarpeyvand, X. Lachenal, P. M. Weaver, Airfoil noise reduction using morphing trailing edge, in: 21st International Congress on Sound and Vibration, 2014.
21. W. Elsahhar, S. A. Showkat Ali, T. Raf, M. Azarpeyvand, An experimental investigation of the effect of bluff body bluntness factor on wake-vortex noise generation, in: 24th AIAA/CEAS Aeroacoustics Conference, AIAA 2018-3288.
22. Y. D. Mayer, H. Kamliya Jawahar, M. Szoke, S. A. Showkat Ali, M. Azarpeyvand, Design and performance of an aeroacoustic wind tunnel facility at the University of Bristol, Applied Acoustics, 155(2019)358-370.
23. X. Liu, S. A. Showkat Ali, M. Azarpeyvand, On the application of trailingedge serrations for noise control from tandem airfoil configurations, in: 23rd AIAA/CEAS Aeroacoustics Conference, AIAA 2017-3716.